EUV Source Development at Energetiq

Paul A Blackborow, Matthew J Partlow, Stephen F Horne, Matthew M Besen, Donald K Smith, Deborah S Gustafson

Energetiq Technology, Inc. Woburn, MA USA

ABSTRACT

As industry advances towards the insertion of EUVL technology, researchers and manufacturers armed with alpha EUV light sources invent an expanding array of potential applications utilizing these sources. This in turn drives development of the light sources to fulfill the large field of specific needs in resist exposure, mirror testing, wafer inspection, etc., which call for a greater variety of source parameters, including output power, source size, and stability.

The EQ-10 is a commercially available, medium-power (10 W/2π, 13.5nm $\pm$1%, Xenon) electrodeless Z-pinch light source.[1] Significant field experience and customer feedback has been accumulated from sources already in operation in multiple locations. In response, a development program is under way to re-engineer and optimize the EQ-10 for a variety of applications. Data will be presented on the effect of varying source geometry, frequency, and input power on pinch performance. We have observed a sustained integrated output power of over 15 Watts. The plasma size can be varied to suit customer applications.

A related program on beamline design and optimization is also underway, focused on debris mitigation while also maintaining the efficiency of EUV power delivery. Initial results from this program will be summarized.

Keywords: Z-Pinch, EUV source, debris mitigation

1. INTRODUCTION

In order for EUV lithography to be a competitive option for semiconductor production, it is crucial for the development of resists and optics that perform at 13.5 nm, as well as debris mitigation techniques, to move forward along with the development of sources for high-volume manufacturing. The current state-of-the-art lithography techniques rely on ArF laser light at 193 nm, a photon energy of only 6.4 eV. With EUV photon energy 92 eV, many times material ionization potentials, the physics dominating the EUV photon interaction with resists and optics is substantially different than that of 193 nm light. While alternative means exist, the most preferred way to test the performance of these components is with an actual EUV light source. EUV light sources are typically one of two types: laser-produced plasma (LPP) and discharge-produced plasma (DPP).[2] Each has its own set of requirements for debris mitigation, which must also be developed in order to scale these sources up for manufacturing.

One commercially available EUV source is the EQ-10, manufactured by Energetiq Technology, Inc. The EQ-10 EUV source produces 10 Watts(2π) of 13.5 nm light in-band ($\pm$1%). Since its introduction, the EQ-10 has been integrated into a number of facilities dedicated to the development of EUV optics and resists. The key unique properties of the source, and references to recent work performed with the EQ-10, are given in the first section below. We then describe the variety of ways we have been able to characterize the source, in more detail than has previously been presented. This includes several markers of source stability. Shifting to beamline design, the next section details our recent work on debris mitigation. Finally, we mention some planned future developments on the EQ-10.

2. ELECTRODLESS Z-PINCH SOURCE DESIGN

The EQ-10 Z-pinch source uses a unique transformer-like design which relies on inductive coupling of current from a low-inductance conductive structure to a plasma secondary. The plasma current flows in closed loops (see Figures 1 and 2)

Further author information:
M.J.P.: E-mail: mpartlow@energetiq.com;
P.A.B.: E-mail: pblackborow@energetiq.com

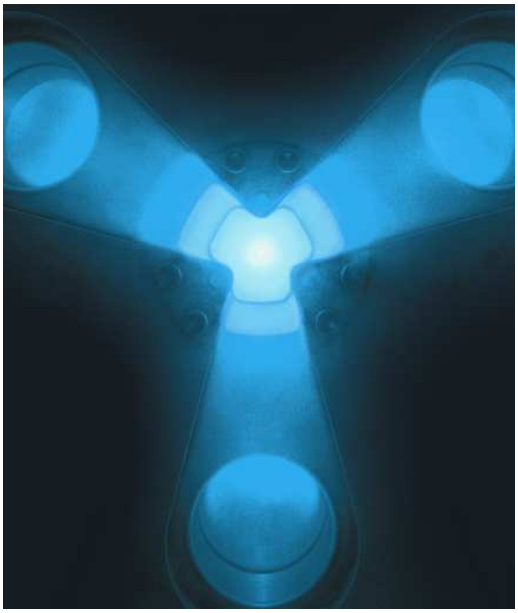

Figure 1: Visible light image of the EQ-10's three plasma loops.

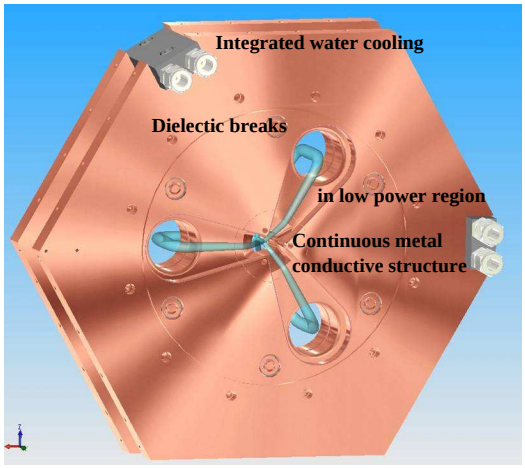

Figure 2: EQ-10 source assembly.

and does not terminate in metal electrodes, thus eliminating the cooling and impurity issues common to the conventional Z-pinch. Details of the source physics, design, and application have been previously published.[1,3]

Our customers have also published a number of papers describing their research conducted utilizing the EQ-10 source, including several in 2007.[4–11]

3. SOURCE PERFORMANCE CHARACTERIZATION

This section begins with a brief description of the metrology tools used to characterize the EQ-10 source. The next section reviews a series of power and size measurements scanning over the source operating range. Lastly, we detail rigorous measurements performed to determine the stability of source operation.

3.1 Metrology

3.1.1 Power Metrology

There are various methods of measuring the EUV output power of the source, several of which had already been described in past publications.[1] A typical arrangement is shown in Figure 3.

The integral components of the power diagnostic are a Ga-As diode and a $\pm 1\%$BW custom[12] 85°mirror. Two Zirconium foils are used to enable *in situ* foil transmission calibration, and a Baratron is used to monitor the pressure of Xenon in the beamline to correct for gas absorption. In practice, a matched pair of photodiode and mirror are calibrated at the SURF facility at NIST, Gaithersburg. The calibration of other power diagnostics are then checked against the NIST calibrated monitor. In addition, we adjust the measurement by taking into account the non-uniform shape of the source spectrum and reflectivity of the mirror around 13.5 nm. However, the adjustment is on the order of 1%.[13]

3.1.2 Size/Position Metrology

To image the EQ-10 source, we use an x-ray pinhole camera and an Andor DO434-BN CCD camera. The apparatus and imaging analysis has been discussed in detail in previous publications.[1] However, some aspects specific to this paper are reviewed below.

We obtain an EUV inband image with the use of a thin Zr foil and an optically flat multilayer mirror acting as spectral filters. With 1 μm thick Zr foils, the necessary exposure time is 0.5 to 1.5 seconds, depending on chosen source operating

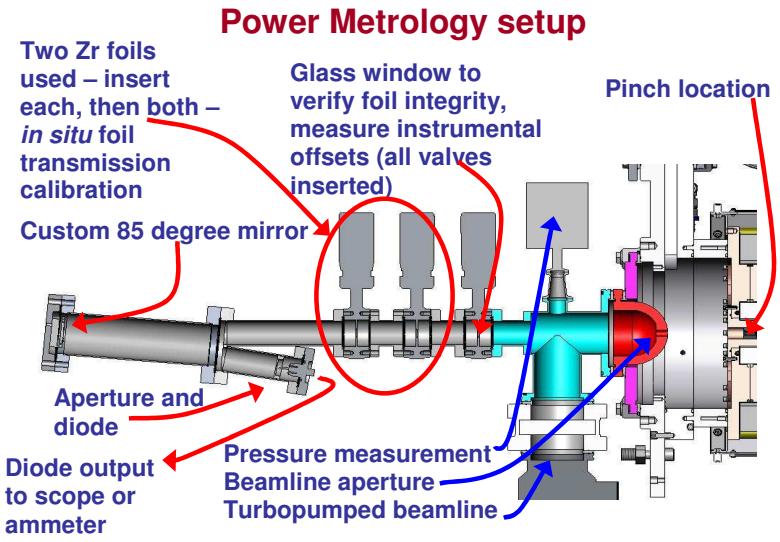

Figure 3: Typical beamline for power metrology using 85°narrow band mirror.

parameters. The imaging system can be controlled by computer and fully automated, so as to capture sequential images over a long time scale of continuous source operation. In order to ensure stability over these long term tests, special care was taken in mounting the imaging beamline to the source. A framework was constructed out of Unistrut that rigidly held the beamline and CCD in place in relation to the source plates, with six contact points to hold against all possible motional degrees of freedom.

3.2 Performance tests on bore/source

The expanding field of specific needs for source performance necessitates a full characterization of the pinch performance, especially in terms of the readily adjustable parameters of input power, pulse frequency, and Xenon pressure. We present below a more thorough investigation of the effects of these parameters on EUV power and size in the EQ-10 source than has been presented in the past.

3.2.1 Power vs. pressure and vs. Frequency

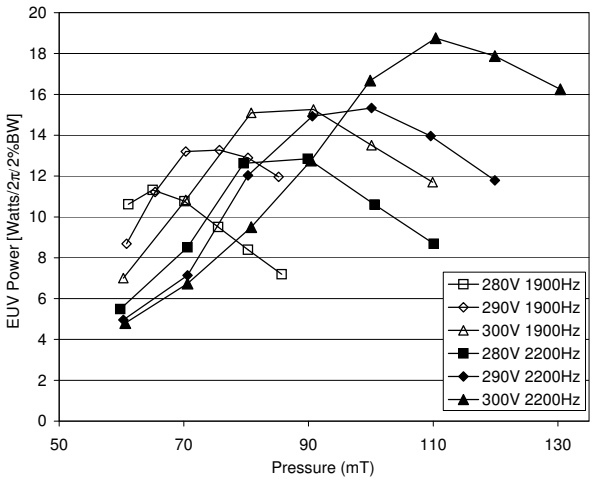

Figure 4: Typical power results in scan of pressure for several voltages and frequencies.

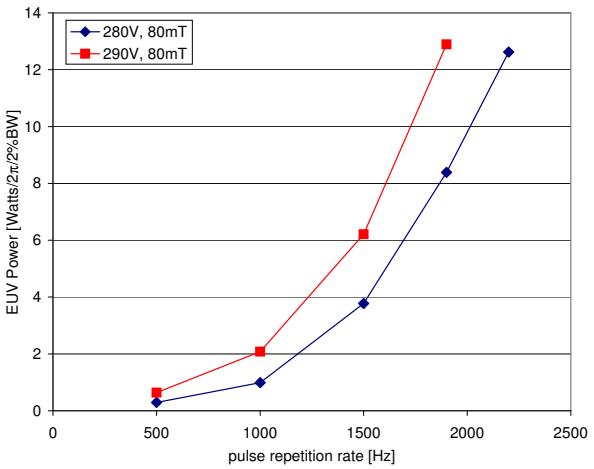

Figure 5: Typical power results in scan of frequency for two source voltages. Source pressure set to 80 mT.

Figure 4 shows typical results for the dependence of EUV output power on source pressure at several values of input power and pulse rate. For any given combination of pulse rate and input power, there exists a unique pressure such that the power is maximized. As expected, this maximum power increases with pulse rate and input power.

The recommended operating settings for the commercial EQ-10 are 280 V for input power and 1900 Hz for pulse rate, chosen to optimize stability and component longevity.

EUV power as a function of pulse rate is shown in Figure 5 over a larger range of frequency than in Figure 4. One might expect the time-averaged (CW) output power to scale linearly with frequency. However, The EUV output power of the pinch is strongly dependent on plasma density. The plasma density is dependent on the temperature within the bore, which also increases with pulse frequency.

3.2.2 Size vs. pressure and vs. frequency

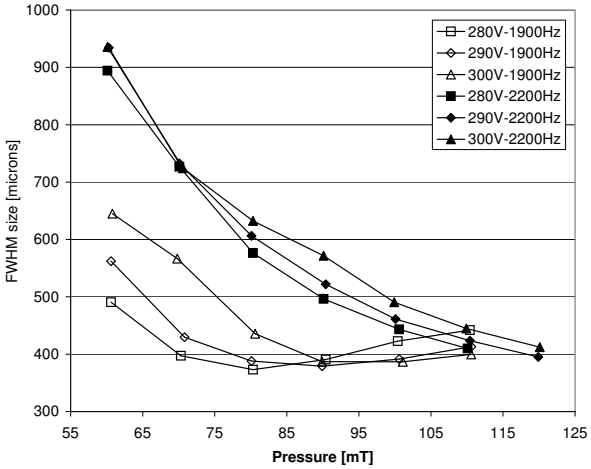

Figure 6: Typical size results in scan of pressure for several voltages and frequencies.

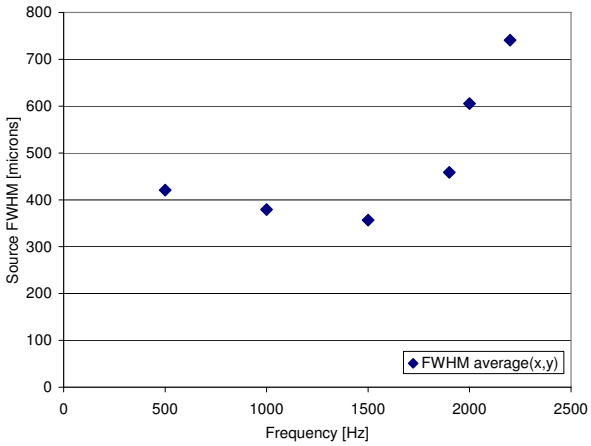

Figure 7: Typical size results in scan of operating frequency. Source pressure set to 80 mT.

Figure 6 shows typical results for the dependence of the EUV pinch size on source pressure at several values of input power and pulse rate. The recommended operating settings for the commercial EQ-10 are 280 V for input power and 1900 Hz for pulse rate, chosen for better stability and component longevity.

EUV size as a function of pulse rate is shown in Figure 7 over a larger range of frequency than in Figure 6. The increase in size with increasing frequency is expected, since as the frequency is increased, and the source temperature increases, the density of the plasma involved in the pinch decreases.

3.3 Stability

Stability in the performance of the source is critical for nearly all applications. Here we present studies of the stability of several key aspects of source performance.

3.3.1 Pulse to Pulse Timing

Using a typical power monitor as described in Section 3.1.2, and a Tektronix 5054B oscilloscope, we measured the distribution, or 'jitter', in the timing between EUV light pulses. A pulse sync signal (SYNC in Figure 8) from the modulator that drives the source served as a trigger. Using the measurement capabilities of the scope, a histogram of the time occurrence of the rising edge of the EUV pulse was recorded, as shown in Figure 9.

For the typical operating conditions of 1900 Hz pulse rate, 280 V input voltage, and 80 mTorr process pressure we measured a standard deviation (σ) of the jitter distribution to be $\sim$57 nanoseconds (6σ = 342 ns) over approximately 3 minutes (a sample size of 6100 pulses).

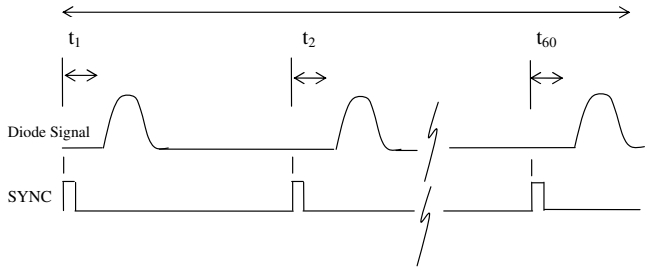

Figure 8: Description of signal used to measure pulse to pulse temporal stability.

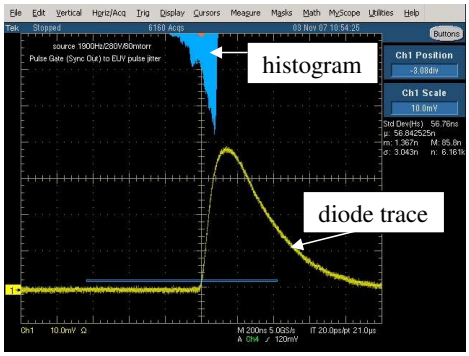

Figure 9: Single diode pulse trace and histogram of pulse edge. Details in text.

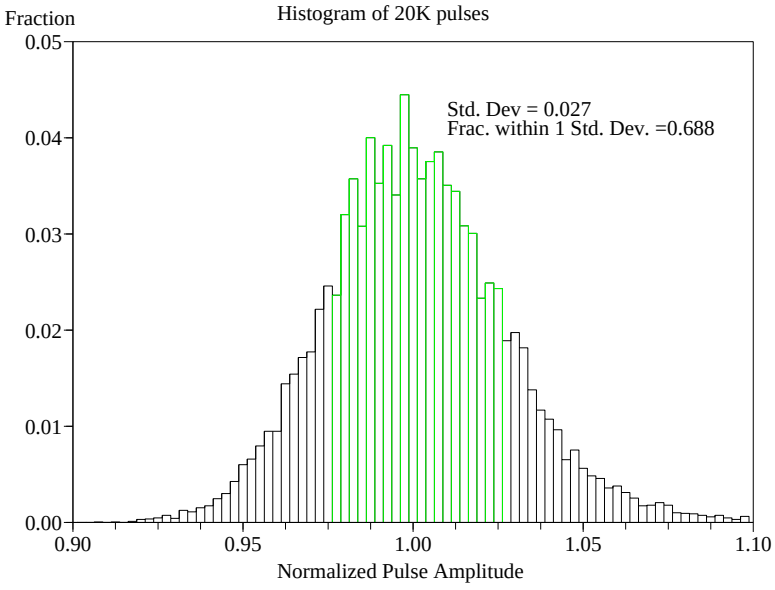

Figure 10: Histogram of pulse intensity of ∼20,000 pulses, demonstrating pulse to pulse stability.

3.3.2 Pulse to Pulse Intensity

The stability in power, or intensity from pulse to pulse, has been measured in two ways. For each, a Stanford Research Systems SR570 low-noise preamplifier with 3 kHz low pass filtering was used to stretch out each EUV pulse for better time resolution.

In the first method, the scope was used to record every single pulse over 10 seconds of continuous source operation. The saved scope trace was then analyzed, with each pulse area being integrated and the distribution of intensities recorded. The result can be seen in Figure 10. Here, the statistics were nearly Gaussian, and the standard deviation σ = 2.7% from the mean intensity.

In the other method, the Tektronix 5054B oscilloscope integrated pulse areas 'on the fly', in this case recording the intensity of every 40th pulse. The statistics of these pulses were recorded for 1 hour, a sample size of 166K. The mean pulse area, μ, was 150.6 μV-sec, with a standard deviation σ = 4.0 μV-sec, giving σ/μ = 2.7%, identical to the other measure.

3.3.3 Position and Size

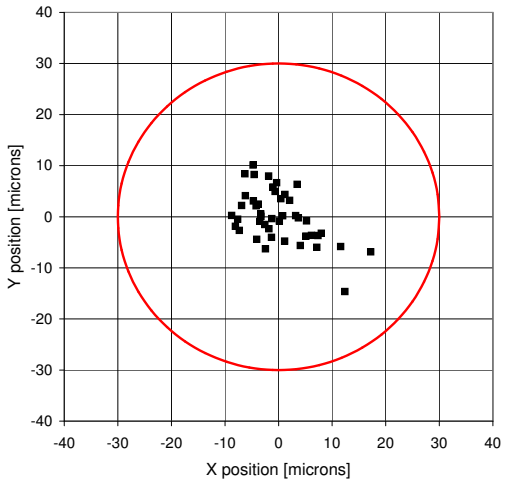

Figure 11: Stability of pinch position over 300 Million pulses continuous operation.

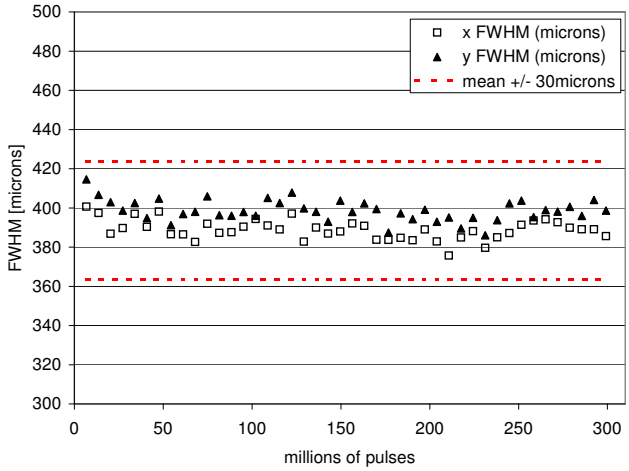

Figure 12: Stability of source size FWHM over 300 Million pulses continuous operation.

Using the the imaging set-up as described in Section 3.1.2, we measured the stability of the position and size of the pinch over various timescales. Figure 11 shows position data in which an image was recorded once an hour for 300 million pulses (roughly 44 hours) of continuous operation. These results are typical, and this measurement has been repeated several times. The statics of the data shown in Figure 11 are σ_x = 5.8 μm and σ_y = 5.0 μm. In a different measurement, an image was recorded every minute for the course of an hour. The statistics of this measurement were σ_x = 3.9 μm and σ_y = 4.1 μm. This is typical of these short term measurements.

From the same imaging data set shown in Figure 11 we have also analyzed the stability of the pinch size over 300 million pulses of continuous source operation. The result is shown in Figure 12. The statistics for the distribution of the size over this 44 hours are an average FWHM of 394 μ with standard deviations σ_{FWHMx} = 5.1 μm and σ_{FWHMy} = 5.5 μm. From the data set of an image recorded every minute for one hour, the statistics were an average FWHM of 378 μ with standard deviations σ_{FWHMx} = 3.1 μm and σ_{FWHMy} = 3.6 μm

Note that in all cases the source was free running. That is, no feedback was being used to control the pressure or input power to the source. Even greater stability could be attained by feedback control of the source pressure (which is currently maintained by a static setpoint on the Xenon mass-flow controller).

4. DEBRIS MITIGATION

Any given plasma source will have a variety of emissions other than the desired EUV photons. Out-of-band photons can be removed by thin spectral filters (typically Zirconium foils). Xenon gas, which attenuates EUV light, can be removed

with appropriate beamline design and choice of vacuum pump. More difficult to remove are fast ions, which may damage optics and other surfaces, and particles from sputtered films, etc, which can also damage beamline components, such as thin foil spectral filters.

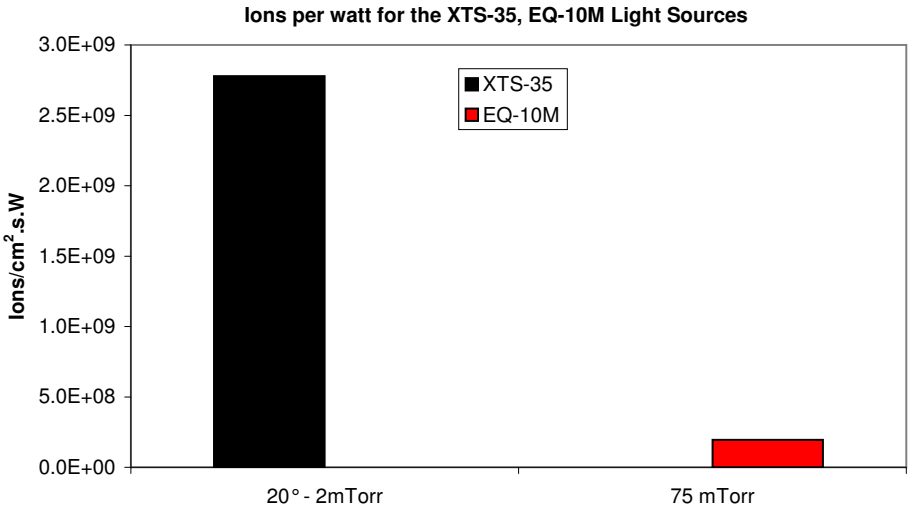

Figure 13: Total integrated adjusted flux at 1.92m. Notice the measurements in the XTS-35 were performed at 20°, while the EQ-10M were performed at 0°. Figure courtesy of C. Castano.[14]

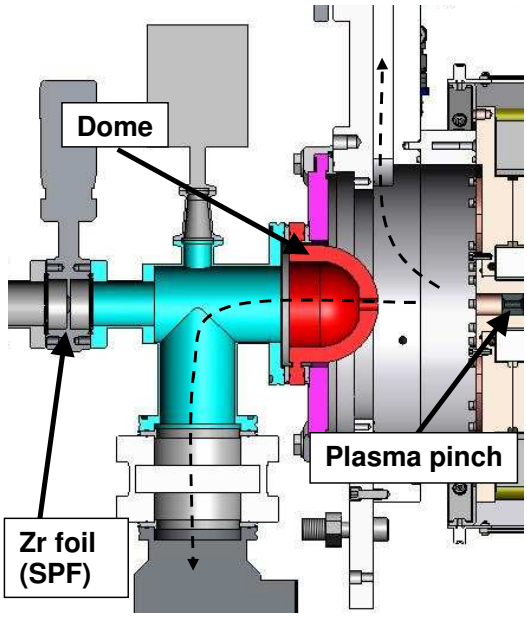

Figure 14: Typical source/beamline arrangement. Dashed lines show direction of gas flow.

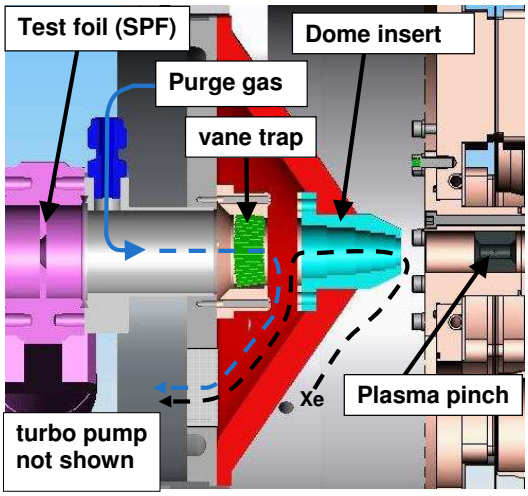

Figure 15: Beamline arrangement to maximize pinch view angle. Dashed lines show direction of gas flow.

The pinch that produces the EUV light also produces highly energetic ions as it expands into the vacuum.[15] Energetic electrons escape rapidly from the plasma pinch, leaving behind a positively charged region which accelerates the multi-charged ions to high energies. Some research has been performed[16] investigating the introduction of light ions to reduce the positive charge left behind after the pinch. However, the EQ-10 source is unique in that the pinch is surrounded by the (relatively) cold plasma of the plasma loops shown in Figure 1, rather than surrounded by vacuum. This cold plasma provides a source of cold electrons which fall into and neutralize the positively charged pinch region. Thus, one would

expect, without any efforts at mitigation, that the EQ-10 would emit less energetic ions than other sources. This was demonstrated in a recent measurement comparing the EQ-10 to another commercially available source, as shown in Figure 13.[14] Note that in this data, the figure of merit being shown is ratio of debris flux to useable EUV light.

Figure 14 shows a typical source-to-beamline configuration we provide to our customers. Here the dome aperture separating the beamline from the source is 10 mm or less in diameter, and located $\sim$ 10 cm from the pinch. The dashed lines show how Xe gas is pumped from the system. The distances and small aperture size minimize the need for particle mitigation, and we have observed long lifetimes ($\sim$ 100 million pulses) for our thin foil spectral purity filters (SPFs), located $\sim$35 cm from the pinch.

However, should a large view angle of the pinch be desired, the arrangement in Figure 14 is insufficient, as it allows a collection angle of about 3°half angle. To achieve a larger collection angle, one needs to move to dome aperture closer to the pinch, as well as increase its diameter. Further modifications to the beamline design are then required, as this change in dome aperture may allow more of the plasma and debris into the beamline, which increases the rate of damage to SPFs and other optics.

Figure 15 shows a prototype design for large angle EUV light collection from the pinch (e.g. to completely fill collection optics).[17] Besides moving and enlarging the dome aperture, a vane trap was placed between the source and beamline, and a mitigation gas flow was introduced between the SPF and the vane trap. Note the change in pumping arrangement, where both the mitigation gas and Xenon are pumped by a single pump attached to the dome. The pumped dome serves as 'barrier' between the source environment and the beamline environment, keeping plasma and Xenon from the beamline, and purge gas from the source. With an appropriately sized SPF at 19 cm from the source, light collection could be from up to $\sim$ 8°half angle.

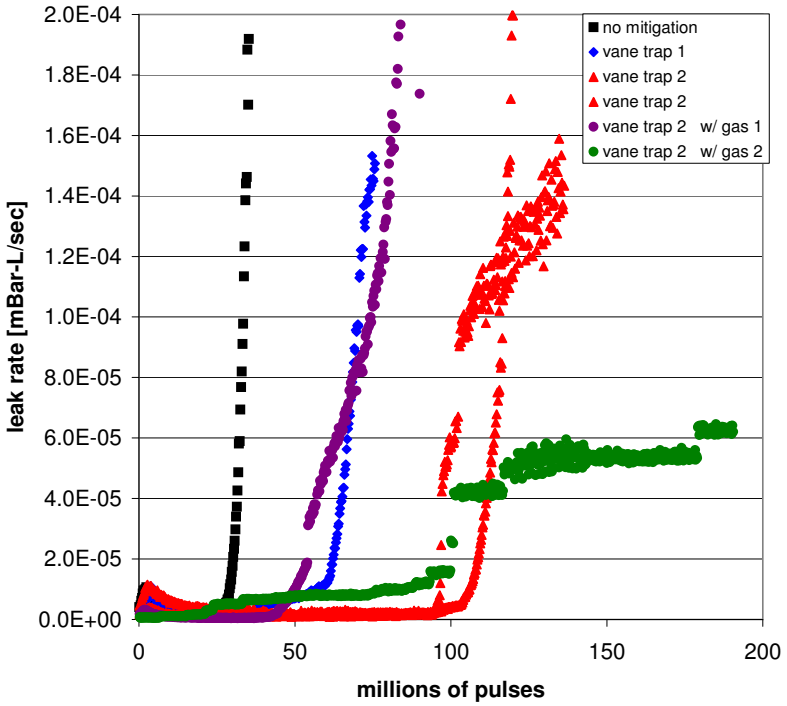

Figure 16: Testing of mitigation techniques with 500 nm thick Aluminum foils.

We tried several combinations of vane traps and purge gases. The figures of merit for initial testing were the temperature of components in the beamline and the change in leak rate across low cost 500 μm thick Aluminum foils. Temperature measurements serve as a measure of plasma entering into the beamline, while foil leak rates give a measure of damage to sensitive optics due to particles or plasma.

The leak rate results are shown in Figure 16. With vane trap 2, and no purge gas flow, the temperature measured in the beamline was 265°C. With vane trap 2 and purge with gas 1, the temperature was 200°C, however, the Al foil failed

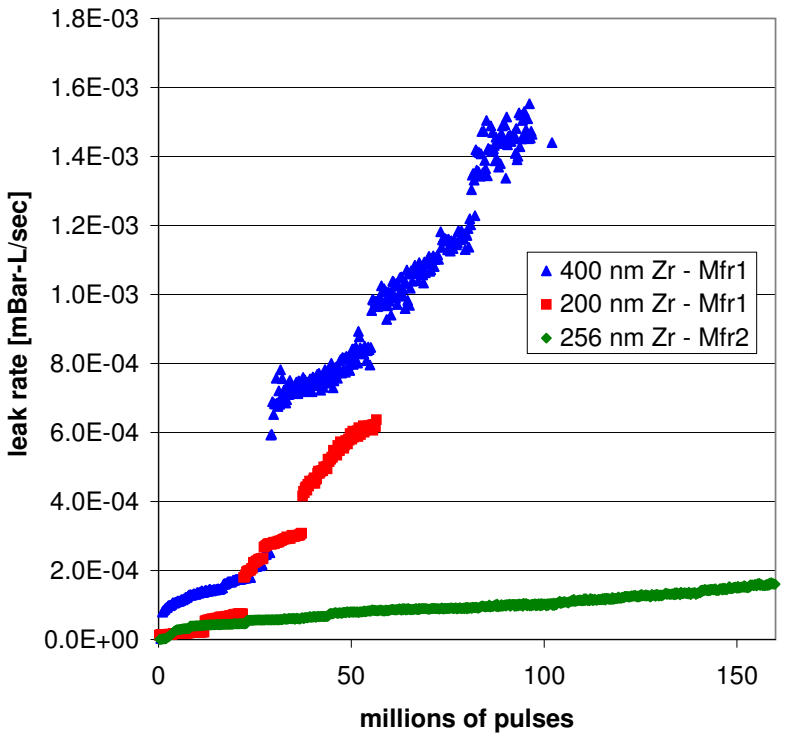

Figure 17: Testing of various Zr foils with a set mitigation scheme.

more rapidly than the foil in the test done without any purge gas. With vane trap 2, and purge gas 2, the temperature in the beamline was 160°C, and the result was acceptable foil lifetimes.

Further tests were then performed with the vane trap 2 and purge gas 2 arrangement and using thin Zirconium foils rather than Aluminum. The results of these test, using foils from two different manufacturers, is shown in Figure 17. Note that, while quantitative comparisons cannot be directly made between the leak rates in Figure 16 and Figure 17 due to the effect of varying types of purge gases and their associated flow rates, all tests shown in Figure 17 were preformed with identical gas/vacuum conditions. The foil made by manufacturer 2 performs the best, with a slow rate of change in leak rate beyond 160 million pulses. After this time, the measured visible light transmission due to pinholes in the foil was $\ll 1\%$ of the total diode signal, agreeing with the open area calculated from the leak rate. Also, the change in EUV transmission through the foil dropped from 22.1% to 19.3% over this 160 million pulses.

5. PLANNED DEVELOPMENTS

Several upgrades to the EQ-10 are currently under development, one of which is briefly discussed below.

5.1 15 Watt source

More available EUV power could yield way to shorter exposure times or more rigorous debris mitigation techniques. There are several ways in which the current version of the EQ-10 can produce greater than 10 Watts/2π/2%BW output power. As evidenced in the survey described in Section 3.2.1, input power and pulse rate can be adjusted to give nearly 20 Watts/2π/2%BW. Figure 18 shows initial testing of the source producing 15 Watts/2π/2%BW, at 280 V input power and 2800 Hz pulse rate, for 2.5 hours of continuous operation, with no heat load issues. Thermal modeling and temperature measurements further imply that source cooling is adequate. However, before a 15W version of the EQ-10 is commercially available, a full program of reliability and lifetime testing must be completed.

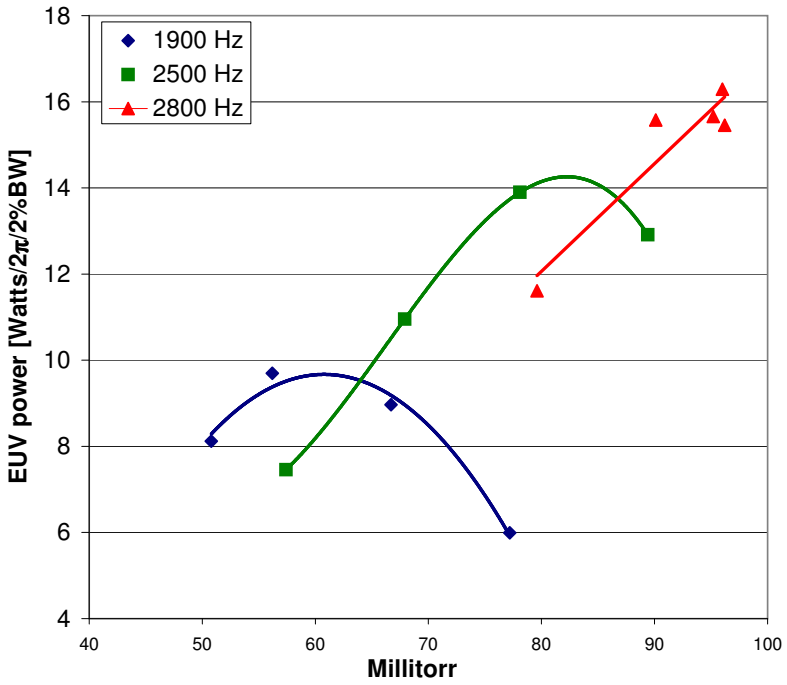

Figure 18: Initial '15 Watt' tests on the EQ-10 R&D source.

6. CONCLUSIONS

As a compact and economic EUV source, the EQ-10 is a versatile tool, which can be used in a variety of studies, including the development of resists and optics for 13.5 nm, and is already being used in several laboratories.[4–11] In repeated studies in our manufacturing facilities, the source has demonstrated reliability in operation and predictable behavior as a function of its operating parameters. Furthermore, rigorous testing has been carried out to place upper limits on the stability of source operation. Beyond source testing, we have recently completed an initial stage in the development of debris mitigation techniques, with positive results, providing customers with a rugged source-to-beamline interface.

The EQ-10 can be modified to produce even greater integrated output power, and continuous operation at 15 Watts has been demonstrated. However, a program of reliability and lifetime study must be completed before the higher power version is commercially available.

REFERENCES

[1] S. F. Horne, M. M. Besen, D. K. Smith, P. A. Blackborow, and R. D'Agostino, "Application of a high-brightness electrodeless Z-pinch EUV source for metrology, inspection, and resist development," in *Emerging Lithographic Technologies X. Edited by Lercel, Michael J. Proceedings of the SPIE, Volume 6151, pp. 201-210 (2006).*, M. J. Lercel, ed., pp. 201–210, Apr. 2006.

[2] V. Bakshi, *EUV Sources for Lithography (SPIE Press Monograph Vol. PM149)*, SPIE- International Society for Optical Engineering, 2006.

[3] P. A. Blackborow, D. S. Gustafson, D. K. Smith, M. M. Besen, S. F. Horne, R. J. D'Agostino, Y. Minami, and G. Denbeaux, "Application of the Energetiq EQ-10 electrodeless Z-Pinch EUV light source in outgassing and exposure of EUV photoresist," in *Emerging Lithographic Technologies XI. Edited by Lercel, Michael J.. Proceedings of the SPIE, Volume 6517, pp. 65171W (2007).*, *Presented at the Society of Photo-Optical Instrumentation Engineers (SPIE) Conference* **6517**, Mar. 2007.

[4] K. R. Dean, I. Nishiyama, H. Oizumi, A. Keen, H. Cao, W. Yueh, T. Watanabe, P. Lacovig, L. Rumiz, G. Denbeaux, and J. Simon, "An analysis of EUV-resist outgassing measurements," in *Advances in Resist Materials and Processing Technology XXIV. Edited by Lin, Qinghuang. Proceedings of the SPIE, Volume 6519, pp. 65191P (2007).*, *Presented at the Society of Photo-Optical Instrumentation Engineers (SPIE) Conference* **6519**, Mar. 2007.

[5] R. Garg, A. Antohe, and G. Denbeaux, "Absorption measurments of extreme ultraviolet radiation in photoresists," in *Emerging Lithographic Technologies XI. Edited by Lercel, Michael J.. Proceedings of the SPIE, Volume 6517, pp. 65172O (2007).*, *Presented at the Society of Photo-Optical Instrumentation Engineers (SPIE) Conference* **6517**, Mar. 2007.

[6] G. Denbeaux, Y. J. Fan, A. Antohe, L. Yankulin, R. Garg, O. Wood, F. Goodwin, C. Koay, K. Goldberg, E. Anderson, and W. Chao, "Actinic microscope for EUV masks using a stand-alone source for imaging and contamination studies of EUV masks," in *International Symposium on Extreme Ultraviolet Lithography, Sapporo, Japan*, Sematech, 2007. Proceedings available from SEMATECH, Austin, TX.

[7] A. Sekiguchi, Y. Kono, M. Kadoi, Y. Minami, T. Kozawa, S. Tagawa, D. Gustafson, and P. Blackborow, "Study on photochemical analysis system (VLES) for EUV lithography," in *Advances in Resist Materials and Processing Technology XXIV. Edited by Lin, Qinghuang. Proceedings of the SPIE, Volume 6519, pp. 651946 (2007).*, *Presented at the Society of Photo-Optical Instrumentation Engineers (SPIE) Conference* **6519**, Mar. 2007.

[8] H. Yamamoto, T. Kozawa, S. Tagawa, K. Ohmori, M. Sato, and H. Komano, "Single component chemically-amplified resist based on dehalogenation of polymer," in *Advances in Resist Materials and Processing Technology XXIV. Edited by Lin, Qinghuang. Proceedings of the SPIE, Volume 6519, pp. 65192G (2007).*, *Presented at the Society of Photo-Optical Instrumentation Engineers (SPIE) Conference* **6519**, Mar. 2007.

[9] J. J. Santillan, M. Toriumi, and T. Itani, "A study of EUV resist outgassing characteristics using a novel outgas analysis system," in *Advances in Resist Materials and Processing Technology XXIV. Edited by Lin, Qinghuang. Proceedings of the SPIE, Volume 6519, pp. 651944 (2007).*, *Presented at the Society of Photo-Optical Instrumentation Engineers (SPIE) Conference* **6519**, Mar. 2007.

[10] J. J. Santillan, S. Kobayashi, and T. Itani, "EUV Resist Outgassing Studies in Selete," in *International Symposium on Extreme Ultraviolet Lithography, Sapporo, Japan*, Sematech, 2007. Proceedings available from SEMATECH, Austin, TX.

[11] H. Yamamoto, T. Kozawa, S. Tagawa, H. Yukawa, M. Sato, and H. Komano, "Effect of Fluorine Atom onAcid Generationin Chemically Amplified EUV Resist," in *International Symposium on Extreme Ultraviolet Lithography, Sapporo, Japan*, Sematech, 2007. Proceedings available from SEMATECH, Austin, TX.

[12] E. Gullickson. personal communication.

[13] S. Horne, M. Partlow, M. Besen, D. Smith, P. Blackborow, and D. Gustafson, "EUV Source Development at Energetiq Technology," in *International Symposium on Extreme Ultraviolet Lithography, Sapporo, Japan*, Sematech, 2007. Proceedings available from SEMATECH, Austin, TX.

[14] C. H. Castano, J. Sporre, K. C. Thompson, S. N. Srivastava, D. N. Ruzic, and V. Bakshi, "Standard Ionic Debris Measurements," in *International Symposium on Extreme Ultraviolet Lithography, Sapporo, Japan*, Sematech, 2007. Proceedings available from SEMATECH, Austin, TX.

[15] P. Mora, "Plasma expansion into a vacuum," *Phys. Rev. Lett.* **90**, p. 185002, May 2003.

[16] D. N. Ruzic, K. C. Thompson, B. E. Jurczyk, E. L. Antonsen, S. N. Srivastava, and J. B. Spencer, " Reduction of Ion Energies From a Multicomponent Z-Pinch Plasma," *IEEE Trans. on Plasma Science* **35**, pp. 606 –613, June 2007.

[17] M. Partlow, S. Horne, M. Besen, D. Smith, P. Blackborow, and D. Gustafson, "Beamline Design for the Energetiq EQ-10 EUV Source," in *International Symposium on Extreme Ultraviolet Lithography, Sapporo, Japan*, Sematech, 2007. Proceedings available from SEMATECH, Austin, TX.